Available online at BCREC website: https://bcrec.id

Bulletin of Chemical Reaction Engineering & Catalysis, 18 (2) 2023, 285-293

Research Article

Synthesis, Structural Characterization, Hirschfeld Surface Analysis and Photocatalytic CO_2 Reduction of Yb(III) Complex with 4-Aacetylphenoxyacetic Acid and 1,10-Phenanthroline Ligands

Xi-Shi Tai[1], Yuan-Fang Wang[1], Li-Hua Wang[2], Xi-Hai Yan[1,*]

[1]College of Chemistry and Chemical Engineering, Weifang University, Weifang 261061, P. R. China.
[2]College of Biology and Oceanography, Weifang University, Weifang 261061, P. R. China.

Received: 5th June 2023; Revised: 13th July 2023; Accepted: 13th July 2023
Available online: 16th July 2023; Published regularly: August 2023

Abstract

A new nine-coordinated Yb(III) complex [YbL_3(Phen)] (**1**) (*HL* = 2-(4-acetylphenoxy)acetic acid (APA), Phen = 1,10-phenanthroline) was synthesized with 2-(4-acetylphenoxy)acetic acid, $YbCl_3.6H_2O$, NaOH and 1,10-phenanthroline as materials. Complex (**1**) was characterized by IR and X-ray single-crystal diffraction analysis. The results show that the Yb(III) ion is nine-coordinated with seven carboxylate oxygen atoms from five different deprotonated APA ligands and two nitrogen atoms from one Phen ligand. Complex (**1**) forms a 3D supramolecular framework through the π-π stacking interactions between the Phen aromatic rings. The Hirschfeld surface analysis of complex (**1**) was also calculated. The CO_2 photoconversion activity of complex (**1**) has been performed under UV-vis light irradiation. The complex (**1**) shows good photocatalytic activity with the yield of CO is closed to 146 μmol/g after three hours of UV-vis light irradiation, the CO selectivity has reached to 97.9%.

Keywords: 2-(4-Acetylphenoxy)acetic acid; Yb(III) complex; Synthesis; Crystal structure; Hirschfeld surface analysis; Photocatalytic CO_2 reduction

How to Cite: X.S. Tai, Y.F. Wang, L.H. Wang, X.H. Yan (2023). Synthesis, Structural Characterization, Hirschfeld Surface Analysis and Photocatalytic CO_2 Reduction of Yb(III) Complex with 4-Aacetylphenoxyacetic Acid and 1,10-Phenanthroline Ligands. *Bulletin of Chemical Reaction Engineering & Catalysis*, 18(2), 285-293 (doi: 10.9767/bcrec.18471)

Permalink/DOI: https://doi.org/10.9767/bcrec.18471

1. Introduction

Rare earth complexes have shown excellent potential applications in many aspects due to their unique electronic properties, such as magnetism and near-infrared luminescence [1], chemo- and stereoselective polymerization of polar divinyl monomers [2], corrosion inhibiting properties [3], organic light-emitting materials [4,5], catalysts [6,7], bioactivities [8,9], *etc*. The ligands containing carboxylate group have always been one of the main ligands used to construct metal complexes because they may be provide monodentate, bidentate, or tridentate coordination modes [10–12]. In addition, 1,10-phenanthroline as a second ligand also plays an important role in the structure and property of the ternary metal complexes [13–15]. In the previous studies of our research group, some ternary metal complexes constructed by ligands containing carboxylate group and 1,10-phenanthroline as a second ligand has been synthesized and structural characterized [16–19]. In order to continue to deeply explore the structure and properties of the ternary metal com-

* Corresponding Author.
Email: taixs@wfu.edu.cn (X.H. Yan);
Telp: +86-536-8785286, Fax: +86-536-8785286

plexes, in this work, a new nine-coordinated Yb(II) complex [YbL_3(Phen)] (**1**) has been synthesized with 2-(4-acetylphenoxy)acetic acid, $YbCl_3.6H_2O$, NaOH and 1,10-phenanthroline as materials. The Hirschfeld surface analysis of complex (**1**) was also calculated. The CO_2 photoconversion activity of complex (**1**) has been performed under UV-vis light irradiation. The Scheme of complex(**1)** is shown in Figure 1.

2. Materials and Methods

2.1 Materials and Measurements

2-(4-Acetylphenoxy)acetic acid, $YbCl_3.6H_2O$, NaOH and 1,10-phenanthroline used in this experiment were directly as received without further purification. IR spectra were recorded on a Tianjin Gangdong FTIR-850 spectrometer using a KBr pellet (range ~4000–400 cm^{-1}) (Tianjin Gangdong Sci. & Tech. Co., Ltd, Tianjin, China). Crystal data of [YbL_3(Phen)] (**1**) were obtained using a Bruker SMART CCD 6000 area detector (Bruker, Billerica, MA, USA). The reactor of photocatalytic CO_2 reduction was sealed and irradiated using a 300 W Xe arc lamp (Beijing Trusttech Co., Ltd (PLS-SXE300). The gas products have been achieved every hour and performed the detection using a gas chromatograph (GC-6890, Purkinje General instrument Co., Ltd., Beijing, China) equipped with Propark Q column with FID detector.

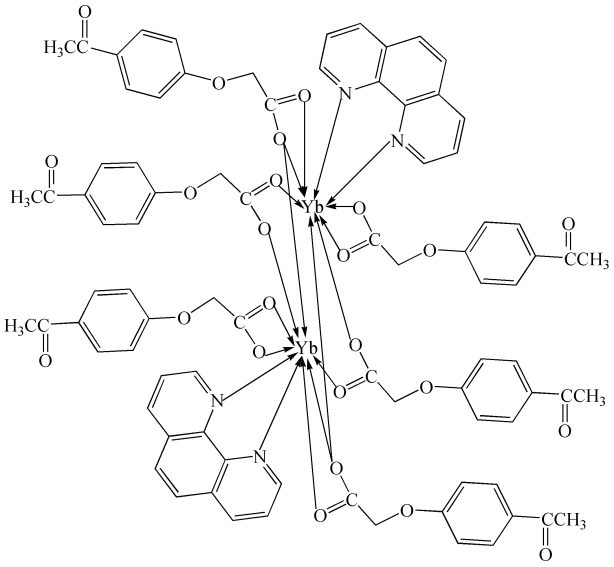

Figure 1. The Scheme of complex (**1**).

2.2 Synthesis of [YbL_3(Phen)] (**1**)

0.0810 g 1,10-phenanthroline (0.50 mmol), 0.1942 g 4-acetylphenoxyacetic acid (1.0 mmol), 0.1937 g $YbCl_3.6H_2O$ (0.50 mmol), and 0.040 g NaOH (1.0 mmol) were added to a solution containing 15 mL 95% ethanol and 15 mL water with stirring. The mixture was heated to 80℃ and the reaction was continued for 6 h. After the reaction was stopped and cooled to room temperature, the above mixture was filtered. The filtrate was transferred to a small beaker and let still at room temperature. Colourless crystals of [YbL_3(Phen)] (**1**) were obtained in 10 days.

2.3 Crystal Structure Determination

A suitable single crystal of complex (**1**) (0.14×0.11×0.09 mm) was used to collect crystal data on a Bruker SMART CCD 6000 area detector equipped with a graphite monochrom-

Table 1. X-ray single-crystal diffraction data for complex (**1**).

Empirical formula	$C_{42}H_{35}N_2O_{12}Yb$
M_r	932.76
T, K	296.15
Crystal system, space group, Z	Triclinic, *P-1*, 2
a, b, c, Å	12.3164(9), 12.7581(9), 14.5023(11)
α, β, γ, deg	70.873(2), 80.281(2), 65.810(2)
V, $Å^3$	1962.4(3)
ρ_{calc}, mg/mm^3	1.579
μ, mm^{-1}	2.449
F(000)	934
h, k, l ranges	$-14 \le h \le 14$, $-15 \le k \le 15$, $-17 \le l \le 17$
Number of reflections: measured (N1), R_{int}/with $I > 2\sigma(I)$ (N2)	44757, 0.0636/6893
Data/restraints/parameters	6893/0/517
S on F^2	1.067
R_1/wR_2 on N1	0.0381/0.0853
R_1/wR_2 on N2	0.0509/0.0906
$\Delta\rho_{min}/\Delta\rho_{max}$, e $Å^{-3}$	−0.49/0.56

ator (MoK_α radiation, λ = 0.71073 Å) at 296.15 K. 6893 unique reflections (R_{int} = 0.0636, R_{sigma} = 0.0543) were used in all calculations for **1**. The structure of complex (**1**) was solved using *SHELXT* program [20] and refined using the *SHELXL* [21] program by full-matrix least-squares method. Coordinates of hydrogen atoms were refined without any constraints or restraints. The hydrogen atoms were positioned geometrically (C−H = 0.93-0.97 Å). Their U_{iso} values were set to 1.2U_{eq} or 1.5U_{eq} of the parent atoms. X-ray single-crystal diffraction data for complex (**1**) are given in Table 1. Molecular structure of complex (**1**) was drawn using Diamond [22]. The Hirschfeld surface analysis of complex (**1**) was calculated by the Crystal Explorer software [23]. Crystallographic data have been deposited with Cambridge Crystallographic Data Centre (CCDC 2205446). A copy of this information may be obtained free of charge from The Director, 12 Union Road Cambridge CB2 1EZ, UK; Fax: 44-1223-336033; e-mail: deposit@ccdc.cam.ac.uk.

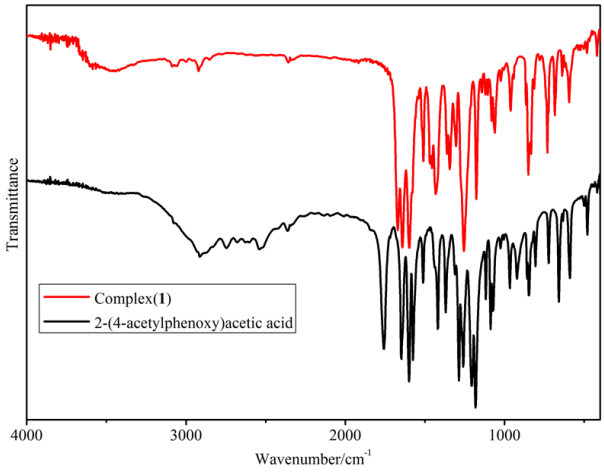

Figure 2. The infrared spectra of 2-(4-acetylphenoxy)acetic acid and the complex (**1**).

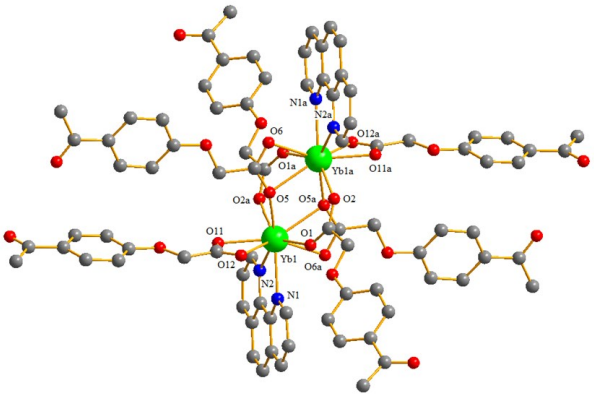

Figure 3. The molecular structure of complex (**1**).

2.4 Photocatalytic CO_2 Reduction Evaluation

The obtained complex (**1**) catalyst (0.05 g) was dispersed into 100 mL H_2O, transferring the suspension solution into a quartz reactor with continuous stirring. The temperature of quartz reactor was controlled at 20 °C. Abundant high purity CO_2 gas was bubbled into the above reactor for 15 min. Subsequently, the reactor was sealed and irradiated using a 300 W Xe arc lamp (Beijing Trusttech Co., Ltd (PLS-SXE300). The gas products have been achieved every hour and performed the detection using a gas chromatograph (GC-6890, Purkinje General instrument Co., Ltd., Beijing, China) equipped with Propark Q column with FID detector.

3. Results and Discussion

3.1 Infrared Spectra

The infrared spectra of 2-(4-acetylphenoxy)acetic acid and the complex (**1**) are shown in Figure 2. In complex (**1**), the bands at 1596 cm^{-1} and 850 cm^{-1} are assigned to ν(C=N) and ν(C=C) of 1,10-phenanthroline, respectively, which show that two N atoms of 1,10-phenanthroline are coordination with ytterbium(III) ion. The 2-(4-acetylphenoxy)acetic acid ligand shows characteristic bands at 1758 (−COOH, ν(C=O)), 1648 (ν_{as}(COO^-)), 1598 (ν_s(COO^-)), and 1286 (ν(C−O)) cm^{-1}, in complex (**1**), the bands appear at 1670 (ν_{as}(COO^-)), 1641 (ν_{as}(COO^-)), 1467 (ν_s(COO^-)), and 1255 (ν(C−O)) cm^{-1}, indicating that the carboxylate of deprotonated 2-(4-acetylphenoxy)acetic acid ligand is coordinated with ytterbium(III) ion. which are consistent with the result of X-ray single-crystal diffraction analysis.

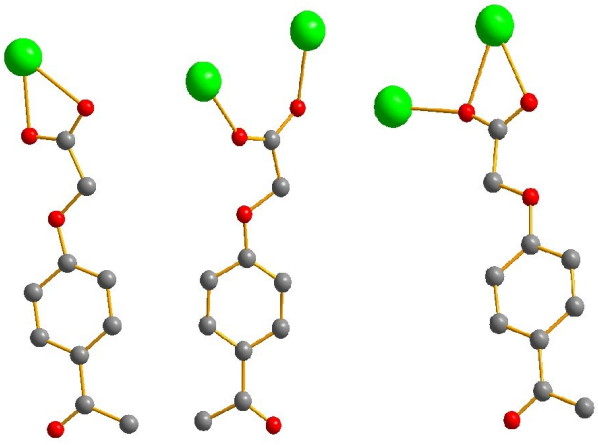

Figure 4. The coordination modes of carboxylates in complex (**1**).

3.2 Structural Description of [YbL3(Phen)] (1)

Single-crystal X-ray diffraction reveals that complex (**1**) crystallizes in the triclinic system with the *P*-1 space group. The asymmetrical unit of complex (**1**) contains one ytterbium(III) ion, three 2-(4-acetylphenoxy)acetic acid (APA) and one 1,10-phenanthroline (Phen). As shown in Figure 3, the ytterbium(III) center is nine-coordinated with seven carboxylate oxygen atoms (O1, O2a, O5, O5a, O6a, O11, O12) from five different deprotonated APA ligands and two nitrogen atoms (N1, N2) from one Phen ligand. The Yb-O and Yb-N distances are in the range of 2.317(5)-2.572(6) Å, which are comparable to other Yb(III)-complexes [24,25]. The selected bond lengths (Å) and angles (°) for complex (**1**) are given in Table 2. The carboxylate of APA ligands possess three different coordination modes (Figure 4): the first is the two oxygen atoms of the deprotonated carboxylate group coordinated with one Yb(III) ion, the second is the two oxygen atoms of the deprotonated carboxylate group coordinated with the different Yb(III) ions, and the third is the two oxygen atoms of the deprotonated carboxylate group coordinated with one Yb(III) ion, and one of the oxygen atoms are further coordinated with another Yb(III) ion. The complex (**1**) formed the binuclear units structure due to the bridge-linking effect of the carboxylate. Through the calculated result of PLATON software, the ring 2 (6-membered ring, C1-C2-C6-C7-C8-C9, belong to the 1,10-phenantroline),

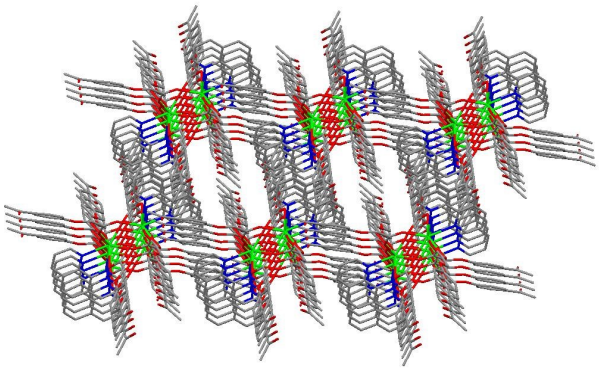

Figure 5. 3D supramolecular framework structure of complex (**1**).

Table 2. Selected bond lengths and angles for complex (**1**).

Bond	Distance, Å	Bond	Distance, Å
Yb1–O1	2.313(3)	Yb1–O2a	2.331(3)
Yb1–O5	2.335(3)	Yb1–O11	2.374(3)
Yb1–O5a	2.518(3)	Yb1–O6a	2.457(3)
Yb1-O12	2.539(4)	Yb1-N1	2.505(4)
Yb1-N2	2.572(4)		
Bond	**Angle, deg**	**Bond**	**Angle, deg**
O1–Yb1–O5	74.59(11)	O5–Yb1–O5a	73.20(12)
O1–Yb1–O5a	70.87(11)	O5–Yb1–O11	86.59(11)
O1–Yb1–O2a	137.88(11)	O5–Yb1–O6a	124.21(11)
O1–Yb1–O11	126.91(12)	O5–Yb1–O12	74.71(11)
O1–Yb1–O6a	77.20(11)	O5a–Yb1–O12	137.41(11)
O1–Yb1–O12	74.16(11)	O5–Yb1–N1	141.47(12)
O1–Yb1–N1	78.36(11)	O5–Yb1–N2	148.34(12)
O1–Yb1–N2	136.91(12)	O5a–Yb1–N2	109.93(11)
O2a–Yb1–O5a	73.41(11)	O2a–Yb1–O11	78.44(12)
O2a–Yb1–O6a	97.91(12)	O2a–Yb1–O12	122.85(12)
O2a–Yb1–N1	141.37(12)	O2a–Yb1–N2	76.59(12)
O5a–Yb1–O11	148.81(11)	O6a–Yb1–O11	147.21(12)
O12–Yb1–O11	52.92(12)	O11–Yb1–N1	88.22(12)
O11–Yb1–N2	75.56(12)	O6a–Yb1–O5a	52.27(10)
O12–Yb1–O6a	139.14(11)	O6a–Yb1–N1	74.34(12)
O6a–Yb1–N2	71.93(12)	O12–Yb1–N2	112.13(12)
O5a–Yb1–N1	122.36(11)	O12–Yb1–N1	71.83(12)
N2–Yb1–N1	64.96(12)		

Symmetry codes: (a) 2 – *x*, 1 – *y*, 1 – *z*.

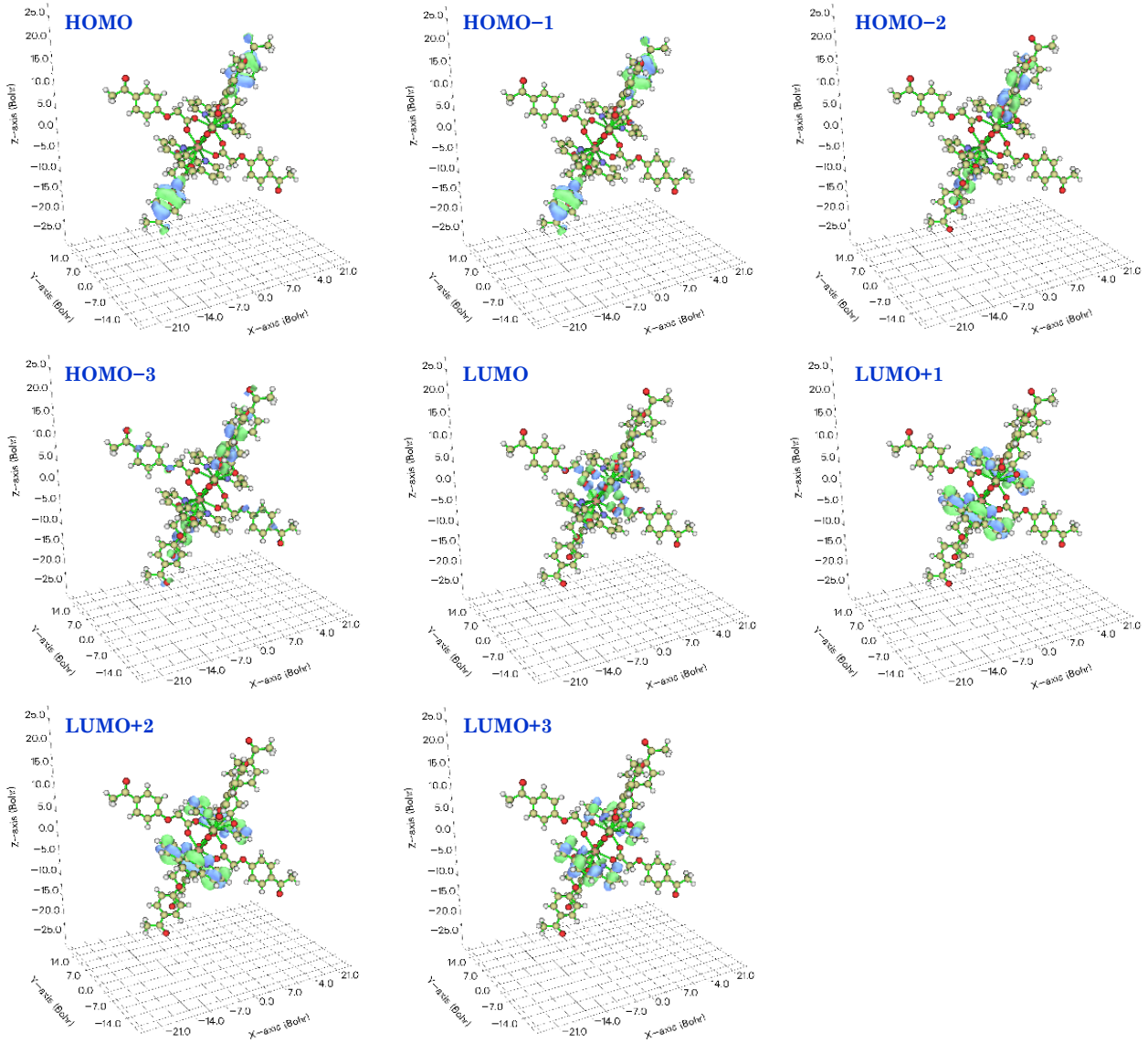

Figure 6. The orbital figures of HOMO, HOMO−1, HOMO−2, HOMO−3, LUMO, LUMO+1, LUMO+2, LUMO+3.

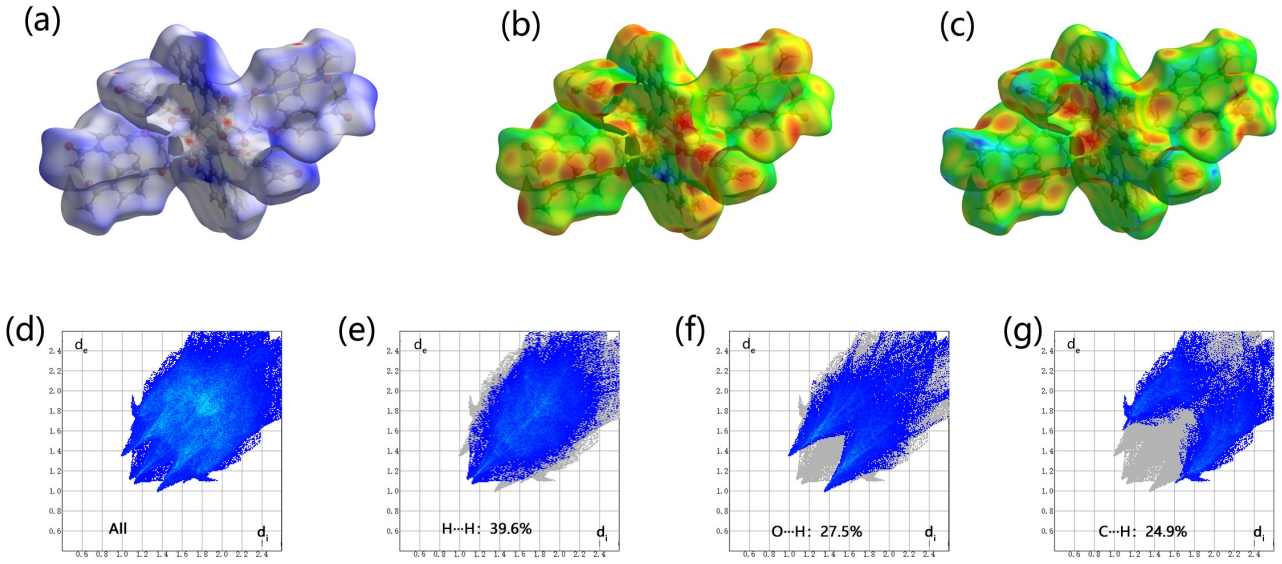

Figure 7. The hirschfeld surface analysis of complex (**1**).

ring 3 (6-membered ring, C15-C16-C17-C18-C19-C20, belong to the 2-(4-acetylphenoxy)acetic acid) and ring 8 (14-membered ring, N1-C9-C1-N2-C5-C4-C3-C2-C6-C7-C8-C12-C11-C10, belong to the 1,10-phenantroline) are responsible for the π-π stacking interaction. They play an important role in forming the 3D supramolecular framework (Figure 5). The detailed π-π stacking interactions data are listed in Table 3.

3.3 Hirschfeld Surface Analysis of [YbL_3(Phen)] (**1**)

To better understand the surface contacts of the crystal, the Hirschfeld surface analysis of the complex (**1**) was calculated by the Crystal Explorer software 21.5. The HOMO and LUMO of the complex are calculated by the Gaussian software [26]. The HOMO energy is −6.161762 eV and the LUMO energy is −5.789377 eV. The orbital figures of HOMO, HOMO−1, HOMO−2, HOMO−3, LUMO, LUMO+1, LUMO+2, LUMO+3 are shown in Figure 6. The Hirschfeld surfaces mapped over dnorm, di and de are shown in Figure 7 (a-c), the two-dimensional (2D) fingerprint plots representing overall and the top three interactions (H···H, O···H/H···O and C···H/H···C) are shown in Figure 7 (d-g). Through the analysis, we can see that the H···H contacts represented the biggest contributions (39.6%) to the Hirschfeld surface, followed by O···H/H···O and C···H/H···C contacts with contributions of 27.5% and 24.9%, respectively. The C···C contacts with a Hirschfeld surface contribution of 4.2%, indicating that the π-π stacking interactions play a subordinate role in forming the crystal (Figure 8).

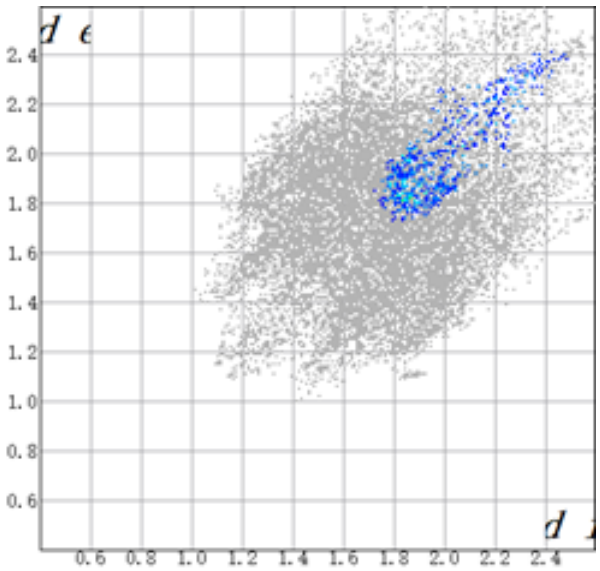

Figure 8. The Hirschfeld surface contribution of π-π stacking interaction.

3.4 Photocatalytic CO_2 Reduction Studies

The CO_2 photoconversion activity of complex (**1**) has been performed under UV-vis light irradiation and the result was displayed in Figure 9. It could be found that complex (**1**) could catalyze CO_2 into CO in the first two hours. With the increase of time, small amounts of methane can be detected, but the selectivity of the product is mainly CO. In the process of photocatalytic CO_2 reduction, reducing CO_2 into CO requires only two electrons, while reducing CO_2 into CH_4 requires eight electrons ($CO_2 + 2H^* + 2e^- \rightarrow CO + H_2O$, $CO_2 + 8H^* + 8e^- \rightarrow CH_4 + 2H_2O$). Therefore, it's harder to get methane products compared to CO. After three hours of UV-vis light

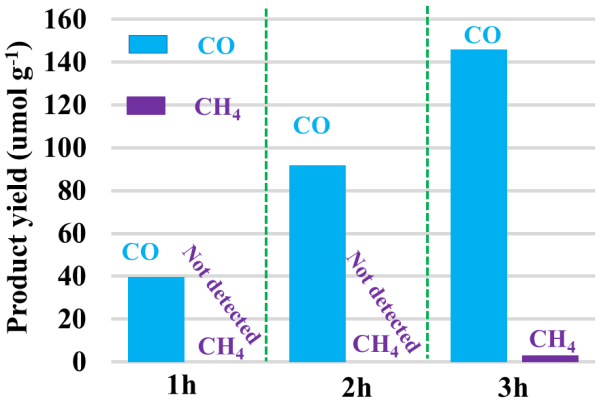

Figure 9. The CO_2 photoconversion activity of complex (**1**) under UV-vis light irradiation.

Table 3. The π-π stacking interactions data of complex (**1**).

Ring plane	Ring plane	Symmetric operation code	Distance between ring centroids (Ang.)	Slippage (Ang.)
Ring 2	Ring 3		3.735(3)	1.359
Ring 2	Ring 8		3.723(3)	1.295
Ring 3	Ring 2	2-x, -y, 1-z	3.736(3)	1.289
Ring 8	Ring 2		3.723(3)	1.296
Ring 8	Ring 8		3.735(3)	1.335

irradiation, the yield of CO is closed to 146 μmol/g, the CO selectivity has reached to 97.9%. The produce of small amount of methane is possibly due to the closed system, which leads to further reduction because of the failure of partial CO desorption in time. Meanwhile, we have summarized the activities of Yb(III) complex and some commonly used photocatalysts, the data is listed in Table 4.

4. Conclusions

In summary, we synthesized and structurally characterized a new nine-coordinated Yb(III) complex. The Hirschfeld surface analysis of the Yb(III) complex was calculated. The photocatalytic CO_2 reduction activity shows that the complex (**1**) as catalyst has good the yield of CO and the CO selectivity.

Acknowledgments

The authors would like to thank the National Natural Science Foundation of China (No. 21171132), the Natural Science Foundation of Shandong (ZR2014BL003), the Project of Shandong Province Higher Educational Science and Technology Program (J14LC01), the Research Fund for the Doctoral Program of Weifang University (NO. 2021BS09) and Science Foundation of Weifang.

CRediT Author Statement

Author Contributions: Xi-Shi Tai and Xi-Hai Yan: Conceptualization, Methodology, Investigation, Resources, Data Curation, Writing, Review. Yuan-Fang Wang and Li-Hua Wang: Investigation, Resources, Writing, Review and Editing, Validation. All authors have read and agreed to the published version of the manuscript.

References

[1] Zhang, X.M., Yin, J., Gao, H.L., Cui, J.Z. (2021). Five new multinuclear rare earth complexes: Magnetism and near-infrared luminescence. *Inorganic Chemistry Communications*, 134, 109062. DOI: 10.1016/j.inoche.2021.109062.

[2] Liu, Z.H., Liu, B., Zhao, Z.F., Cui, D.M. (2021). Chemo- and stereoselective polymerization of polar divinyl monomers by rare-earth complexes. *Macromolecules*, 54, 3181-3190. DOI: 10.1021/acs.macromol.1c00009.

[3] Mottram, E., Hamilton, S., Moon, J.S., Wang, J., Bousrez, G., Somers, A.E., Deacon, G.B., Junk, P.C. (2020). Synthesis, structure, and corrosion inhibiting properties of phenylacetato-rare earth(III) complexes. *Journal of Coordination Chemistry*, 73, 2677-2697. DOI: 10.1080/00958972.2020.1839894.

[4] Wang, L.D., Fang, P.Y., Zhao, Z.F., Huang, Y.Y., Liu, Z.W., Bian, Z.Q. (2022). Rare earth complexes with 5d–4f transition: new emitters in organic light-emitting diodes. *The Journal of Physical Chemistry Letters*, 13, 2686-2694. DOI: /10.1021/acs.jpclett.2c00400.

[5] Zhao, Z.F., Wang, L.D., Zhan, G., Liu, Z.W., Bian, Z.Q., Huang, C.H., (2021). Efficient rare earth cerium(III) complex with nanosecond d–f emission for blue organic light-emitting diodes. *National Science Review*, 8, nwaa193. DOI: 10.1093/nsr/nwaa193.

[6] Lyubov, D.M., Tolpygin, A.O., Trifonov, A.A., (2019). Rare-earth metal complexes as catalysts for ring-opening polymerization of cyclic esters. *Coordination Chemistry Reviews*, 392, 83-145. DOI: 10.1016/j.ccr.2019.04.013.

[7] Ren, W.H., Liu, H., You, F., Mao, P.J., So, Y.M., Kang, X.H., Shi, X. C. (2021). Unsymmetrical diarylamido-based rare-earth alkyl complexes: their synthesis and catalytic performance in isoprene polymerization. *Dalton Transactions*, 50, 1334-1343. DOI: 10.1039/D0DT04040A.

Table 4. Comparison of common photocatalysts for CO_2 reduction activity.

References	Sample	CO Yield ($\mu mol.g^{-1}.h^{-1}$)
[27]	g-C_3N_4	1.8
[27]	Cu atom/ g-C_3N_4	3.1
[28]	BiOI	5.18
[29]	La-TiO_2	3.5
[30]	TiO_{2-x}/g-C_3N_4	77.8
[31]	Bi_2WO_6	7.12
[32]	porphyrin MOF	6.88
[33]	NH_2-MIL-125(Ti)	8.25
This work	Yb(III) complex	48.7

[8] Yu, K., Tian, C.C., Li, X., Liao, X.P., Shi, B. (2018). Synthesis, characterization, and antibacterial activity of rare earth-catechin complexes. *Acta Physico-Chimica Sinica*, 34, 543-550. DOI: 10.3866/PKU.WHXB201709291

[9] Guerra, B.R., Glico, A.D., Fernanda de Campos Fraga-Silva, T., Aguiar, J., Venturini, J., Bannach, G. (2021). Rare-earth complexes with anti-inflammatory drug sulindac: Synthesis, characterization, spectroscopic and *in vitro* biological studies. *Inorganica Chimica Acta*, 526, 120516. DOI: 10.1016/j.ica.2021.120516.

[10] Cao, S.H., Tai, X.S., Xin, C.L. (2021). Synthesis, crystal structure and antitumor activity of a Ca(II) coordination polymer based on 4-acetylphenoxyacetate ligands. *Chinese Journal of Structural Chemistry*, 40, 324-328. DOI: 10.14102/j.cnki.0254-5861.2011-2860.

[11] Tai, X.S., Liang, L., Li, X.T., Cao, S.H., Wang, L.H. (2021). Crystal structure of diaqua-bis(μ2-6-phenylpyridine-2-carboxylate-κ3N,O:O)-bis(6-phenylpyridine-2-carboxylato-κ2N,O)lead(II)-N,N-dimethylformamide-water (1/2/4), $C_{54}H_{58}N_6O_{16}Pb_2$. *Zeitschrift für Kristallographie. New Crystal Structures*, 236, 1199-1201. DOI: 10.1515/ncrs-2021-0277

[12] Tai, X.S., Kong, F.Y., Zhou, X.J., Xia, Y.P. (2022). Synthesis, structural characterization and fluorescent property of Cd(II) coordination polymer based on *N*-nicotinoylglycine ligand. *Crystallography Reports*, 67, 209-213. DOI: 10.1134/S1063774522020225

[13] Zhang, L.L., Tang, S.L., Li, D.J., Cheng, Y.Z., Zhang, L.P. (2021). Synthesis and crystal structure of one new Pb(II) complex constructed by 1,10-phenanthroline and two carboxylate ligands. *Main Group Metal Chemistry*, 44, 157-164. DOI: 10.1515/mgmc-2021-0019

[14] Uflyand, I.E., Tkachev, V.V., Zhinzhilo, V.A., Dzhardimalieva, G.I. (2021). Study of the products of the reaction of cobalt(II) acetate with 2-iodoterephthalic acid and 1,10-phenanthroline. *Journal of Coordination Chemistry*, 74, 649-662. DOI: 10.1080/00958972.2021.1881067.

[15] Naso, L.G., Martínez Medina, J.J., D'Alessandro, F., Rey, M., Rizzi, A., Piro, O.E., Echeverría, G.A., Ferrer, E.G., Williams, P.A.M. (2020). Ternary copper(II) complex of 5-hydroxytryptophan and 1,10-phenanthroline with several pharmacological properties and an adequate safety profile. *Journal of Inorganic Biochemistry*, 204, 110933. DOI: 10.1016/j.jinorgbio.2019.110933.

[16] Wang, L.H., Tai, X.S., Ren, X.J. (2022). The crystal structure of [(1,10-phenanthroline-k²N,N)-bis(6-phenylpyridine-2-carboxylate-k2N,O)nickel(II)] monohydrate, $C_{36}H_{26}N_4O_5Ni$. *Zeitschrift für Kristallographie. New Crystal Structures*, 237, 377-379. DOI: 10.1515/ncrs-2022-0046.

[17] Tai, X. S., Wang, Z.J., Ouyang, J., Li, Y.F., Zhang, W., Jia, W.L., Wang, L.H. (2021). The crystal structure of [(phenantroline-k²N,N')-bis(6-phenylpyridine-2-carboxylate-k²N,O)cobalt(II)]monohydrate, $C_{36}H_{26}N_4O_5Co$. *Zeitschrift für Kristallographie. New Crystal Structures*, 236, 1309-1311. DOI: 10.1515/ncrs-2021-0319.

[18] Wang, L.H., Li, P.F. (2018). Synthesis, structure, and catalytic activity of a new Mn(II) complex with 1,4-phenylenediacetic acid and 1,10-phenanthroline. *Bulletin of Chemical Reaction Engineering & Catalysis*, 13, 1-6. DOI: 10.9767/bcrec.13.1.975.1-6.

[19] Zhao, M.L., Tai, X.S. (2022). The crystal structure of phenantroline-k²N,N'-bis(6-phenylpyridine-2-carboxylato-k²N,O)copper(II), $C_{36}H_{24}N_4O_4Cu$. *Zeitschrift für Kristallographie. New Crystal Structures*, 237, 573-575. DOI: 10.1515/ncrs-2022-0121.

[20] Sheldrick, G.M. (2015). *SHELXT*-Integrated space-group and crystal-structure determination. *Acta Crystallographica*, A71, 3-8. DOI: 10.1107/S2053273314026370.

[21] Sheldrick, G.M. (2015). Crystal Structure Refinement with *SHELXL*. *Acta Crystallographica*, C71, 3-8. DOI: 10.1107/S2053229614024218.

[22] Brandenburg, K. (2012). DIAMOND. Visual Crystal Structure Information System. Ver. 3.2; Crystal Impact: Bonn, Germany.

[23] Spackman, P.R., Turner, M.J., McKinnon, J.J., Wolff, S.K., Grimwood, D.J., Jayatilaka, D., Spackman, M.A. (2021). CrystalExplorer:a program for Hirshfeld surface analysis, visualization and qu-antitative analysis of molecular crystals. *Journal of Applied Crystallography*, 54, 1006-1011. DOI: 10.1107/S1600576721002910.

[24] Ye, J.W., Zhang, J.Y., Ning, G.L., Tian, G., Chen, Y., Wang, Y. (2008). Lanthanide coordination polymers constructed from dinuclear building blocks: novel structure evolution from one-dimensional chains to three-dimensional architectures. *Crystal Growth & Design,* 8, 3098-3106. DOI: 10.1021/cg800310j

[25] Wang, L., Li, W.X., Gu, X.M., Zhang, W.L., Ni, L. (2017). Structure variation from one-dimensional chain to three-dimensional architecture: effect of ligand on construction of lanthanide coordination polymers. *Journal of Chemical Sciences*, 129, 271-280. DOI: 10.1007/s12039-017-1225-2.

[26] Frisch, M.J., Trucks, G.W., Schlegel, H.B., Scuseria, G.E., Robb, M.A., Cheeseman, J.R., Scalmani, G., Barone, V., Petersson, G.A., Nakatsuji, H., Li, X.; Caricato, M., Marenich, A.V., Bloino, J., Janesko, B.G., Gomperts, R., Mennucci, B., Hratchian, H.P., Ortiz, J.V., Izmaylov, A.F., Sonnenberg, J.L., Williams Young, D., Ding, F., Lipparini, F., Egidi, F., Goings, J., Peng, B., Petrone, A., Henderson, T., Ranasinghe, D., Zakrzewski, V. G., Gao, J., Rega, N., Zheng, G., Liang, W., Hada, M., Ehara, M., Toyota, K., Fukuda, R., Hasegawa, J., Ishida, M., Nakajima, T., Honda, Y., Kitao, O., Nakai, H., Vreven, T., Throssell, K., Montgomery Jr., J.A., Peralta, J.E., Ogliaro, F., Bearpark, M.J., Heyd, J.J., Brothers, E.N., Kudin, K.N., Staroverov, V.N., Keith, T.A., Kobayashi, R., Normand, J., Raghavachari, K., Rendell, A.P., Burant, J.C., Iyengar, S.S., Tomasi, J., Cossi, M., Millam, J. M., Klene, M., Adamo, C., Cammi, R., Ochterski, J.W., Martin, R.L., Morokuma, K., Farkas, O., Foresman, J.B., Fox, D.J. (2019). Gaussian 16, Revision C.01, Gaussian, Inc., Wallingford CT.

[27] Li, Y., Li, B.H., Zhang, D.N., Cheng, L., Xiang, Q.J. (2020). Crystalline carbon nitride supported copper single atoms for photocatalytic CO_2 reduction with nearly 100% CO selectivity. *ACS Nano*, 14, 10552-10561. DOI: 10.1021/acsnano.0c04544.

[28] Ye, L.Q., Jin, X.L., Ji, X.B., Liu, C., Su, Y.R., Xie, H.Q., Liu, C. (2016). Facet-dependent photocatalytic reduction of CO_2 on BiOI nanosheets. *Chemical Engineering Journal*, 291, 39-46. DOI: 10.1016/j.cej.2016.01.032.

[29] Liu, Y., Zhou, S., Li, J., Wang, Y., Jiang, G., Zhao, Z., Liu, B., Gong, X., Duan, A., Liu, J., Wei, Y., Zhang, L. (2015). Photocatalytic reduction of CO_2 with water vapor on surface La-modified TiO_2 nanoparticles with enhanced CH_4 selectivity. *Applied Catalysis B: Environmental*, 168-169, 125-131. DOI: 10.1016/j.apcatb.2014.12.011.

[30] Shi, H., Long, S., Hu, S., Hou, J., Ni, W., Song, C., Li, K., Gurzadyan, G.G., Guo, X. (2019). Interfacial charge transfer in 0D/2D defect-rich heterostructures for efficient solar-driven CO_2 reduction. *Applied Catalysis B: Environmental*, 245, 760-769. DOI: 10.1016/j.apcatb.2019.01.036.

[31] Liu, Y.P., Shen, D.Y., Zhang, Q., Lin, Y., Peng, F. (2021). Enhanced photocatalytic CO_2 reduction in H_2O vapor by atomically thin Bi_2WO_6 nanosheets with hydrophobic and nonpolar surface. *Applied Catalysis B: Environmental*, 283, 119630. DOI: 10.1016/j.apcatb.2020.119630.

[32] Zheng, C., Qiu, X.Y., Han, J.Y., Wu, Y.F., Liu, S.Q. (2019). Zero-dimensional-g-CNQD-coordinated two-dimensional porphyrin MOF hybrids for boosting photocatalytic CO_2 reduction. *ACS Applied Materials & Interfaces*, 45, 42243-42249. DOI: 10.1021/acsami.9b15306.

[33] Cheng, X.M., Dao, X.Y., Wang, S.Q., Zhao, J., Sun, W.Y. (2021). Enhanced photocatalytic CO_2 reduction activity over NH_2-MIL-125(Ti) by facet regulation. *ACS Catalysis*, 11, 650-658. DOI: 10.1021/acscatal.0c04426.